Improved double-folding α-nucleus potential by including nuclear medium effects

Daming Deng[1,*] and Zhongzhou Ren[1,2,3,4,†]

[1]*Key Laboratory of Modern Acoustics and Department of Physics, Nanjing University, Nanjing 210093, China*

[2]*School of Physics Science and Engineering, Tongji University, Shanghai 200092, China*

[3]*Center of Theoretical Nuclear Physics, National Laboratory of Heavy-Ion Accelerator, Lanzhou 730000, China*

[4]*State Key Laboratory of Theoretical Physics, Institute of Theoretical Physics, Chinese Academy of Science, Beijing 100190, China*

(Received 3 August 2017; published 5 December 2017)

The nuclear medium effect in α decay is introduced into the microscopic double-folding model to construct an improved α-nucleus potential. Under the local density approximation, the α-cluster density distribution is considered to vary with the surrounding matter density as a result of the medium effect. The density-dependence of the α cluster is incorporated by the width parameter of the Gaussian function and constrained by the critical features derived from previous microscopic studies. The influence of the medium effect to the geometry of the α-nucleus potential is studied by comparing with the conventional double-folding potential. To examine the improved potential, the α-decay half-lives and preformation factors of even-even spherical nuclei are calculated and compared with experimental data. With the α-decay data being well explained, it is concluded that the inclusion of the nuclear medium effect contributes to an improved double-folding α-nucleus potential, which incorporates more details of the α-decay process.

DOI: 10.1103/PhysRevC.96.064306

I. INTRODUCTION

Radioactive α decay has long been a powerful tool for studies of nuclear structure. As a fundamental decay mode of unstable nuclei, α decay is directly associated with some of the most exciting subjects in contemporary nuclear physics, such as synthesis and identification of superheavy nuclei [1,2], cluster structure in heavy nuclei [3,4], and exotic properties of drip-line nuclei [5–7]. Theoretical research on α decay is of vital importance to understanding the connection between experimental observables and various nuclear structural properties of our interest.

The cluster model, with an α-core configuration assumed for the α emitter, has been proven very effective in explaining the existing α-decay experimental data. The most crucial ingredient in the cluster model is the adopted α-nucleus interaction. Extensive calculations have been conducted by using different α-nucleus potentials to give quantitative descriptions of α-decay half-lives [8–16]. In these calculations, the α-nucleus potentials are determined through either a phenomenological or a microscopic procedure. The double-folding model, which integrates the density distributions of the α and daughter clusters with realistic nucleon-nucleon (NN) interactions, is a typical representative of the latter. In the previous systematic calculations, the cluster model using the microscopic double-folding potential successfully reproduces the experimental half-lives within a factor of 2–3 [17,18]. Based on its reliability, the model is also exploited to extract useful nuclear structural information, such as nuclear deformation parameters [19,20], charge root mean square (r.m.s.) radius [21,22], and α-preformation factors [23,24]. All these confirm that the microscopic double-folding model provides a reliable description for the effective α-nucleus potential.

Despite the success of the cluster-model approaches mentioned above, there is still an appreciable deviation between the absolute α-decay widths and the theoretical predictions. The discrepancy is usually attributed to the uncertainty of the α-preformation factor (P_α), which is associated with the weight of α-cluster configuration in the initial state of parent nuclei. Unfortunately, it is extremely complicated to microscopically describe the α-formation process in heavy nuclei. Neither the detailed correlations between the cluster nucleons are well understood, nor would it be easy to interpret the preformation mechanism with a microscopic many-body method. To date, a fully microscopic description of α-decay process with self-consistent α-preformation factors remains an open challenge for nuclear physicists. Important progress has been made for typical nuclei such as ^{212}Po [4]. However, for most cases, as an alternative method to obtain the information of α-preformation factor, the P_α factors are extracted from the deviation between theoretical and experimental decay widths, which, however, depends highly on the α-nucleus interaction. Therefore, a highly precise α-nucleus potential is required when determining the magnitude and evolution of the exact P_α factors.

Recently, Röpke *et al.* proposed a microscopic description of the α-formation process and performed an exploratory calculation for the nucleus ^{212}Po [25]. The calculation was then improved by Xu *et al.* [26], in which the Woods-Saxon mean-field potential is replaced by a double-folding α-nucleus potential with measured density distributions for the ^{208}Pb core. Within their description, the α cluster is formed at a critical nuclear density, where the four nucleons of relevance transform from a unbound shell-model state to a bound cluster state. As the α cluster moves towards the nuclear surface with decreasing baryon density, there exists a microscopic process that the cluster simultaneously reduces its size until it

*dengdaming@smail.nju.edu.cn

†zren@nju.edu.cn

finally becomes an α particle. Such an interesting phenomenon is considered as a medium effect, which results from the variation of Pauli blocking. In fact, the medium effect of α cluster was already pointed out in a number of studies that are focused on the clustering phenomenon in nuclear matter [27–32]. However, there is little research on the medium effect in α decay because clustering in nuclei is usually difficult to be described. Although the medium effect only manifests as a subtle change in the cluster size, one should realize that the equivalent change of its density distribution could probably affect the behavior of the resulting α-nucleus potential in the double-folding model. Furthermore, it has been well understood that the α-decay rate is extremely sensitive to the α-nucleus potential, especially the surface region where the medium effect is evident. Thus, in view of its possible importance to a precise α-nucleus interaction, the nuclear medium effect should be taken into account as to the variation of α-cluster density distribution during the α decay process.

To be consistent with the microscopic description of α clustering in nuclei, in the present work we originally introduce this medium effect into the well-known double-folding model. The typical Gaussian density distribution of the α cluster is now considered to be dependent on its surrounding matter density under local density approximation (LDA). A simple formula for this density dependence is proposed, and the resulting influence on the α-nucleus potential is carefully investigated. Additionally, in order to evaluate the overall impact of the medium effect, the α-decay half-lives as well as the preformation factors are calculated with the improved α-nucleus potential. Results are discussed in detail by comparing with the latest experimental data.

The paper is organized as follows. In Sec. II, we briefly outline the modification made to the α-decay double-folding model due to the inclusion of the medium effect. In particular, we will focus on the determination of the density-dependent behavior of the α-cluster density distribution. In Sec. III, correlations between the medium effect and double-folding α-nucleus potential are analyzed. The results of the calculated half-lives and preformation factors are presented and discussed through comparisons with the experiment and those calculated from the traditional double-folding potential. Major influence due to the medium effect is addressed. A summary is given in Sec. IV.

II. THEORETICAL DESCRIPTIONS

A. Inclusion of nuclear medium effect in α-decay double-folding model

The double-folding model was originally proposed for explaining the heavy-ion collision experiments [33] and later applied to α decay and cluster radioactivity [12,13,34]. The mathematical formalism of double-folding potential is derived from the real part of nuclear optical potential, which doubly folds the density distributions of two interactive clusters with effective NN interactions.

$$V_{N,C}(\mathbf{R}) = \lambda \int d\mathbf{r_1} d\mathbf{r_2} \rho_1(\mathbf{r_1}) \rho_2(\mathbf{r_1}) \upsilon(\mathbf{s}). \tag{1}$$

For the Coulomb potential, the effective NN interaction $\upsilon(\mathbf{s} = |\mathbf{R} + \mathbf{r_2} - \mathbf{r_1}|)$ is known analytically, while for the nuclear part it is usually chosen differently according to the case in study. For α decay, the Michigan three-range Yukawa (M3Y) interaction supplemented by a zero-range pseudopotential is a frequent choice for generating the nuclear interaction of the effective α-nucleus potential, which in systematic calculations [17,18], is widely employed to reproducing the experimental α-decay half-lives. In the present study, we use the M3Y-Reid NN interaction, which has the following form:

$$\upsilon(\mathbf{s}, E_\alpha)^{M3Y} = 7999 \frac{\exp(-4s)}{4s} - 2134 \frac{\exp(-2.5s)}{2.5s} + J_{00}(E_\alpha)\delta(\mathbf{s}). \tag{2}$$

Note that the zero-range pseudopotential (i.e., the last term in Eq. (2) with $J_{00}(E_\alpha) = -276(1 - 0.005E_\alpha/A_\alpha)$ MeVfm^3) is introduced to incorporate the single-nucleon exchange effect, where E_α and A_α are the energy and the mass number of the α cluster, respectively. In addition, to obtain the final nuclear potential, the factor λ is necessary to renormalize the strength of the effective NN interaction ($\lambda = 1$ for the Coulomb potential), and it is not an adjustable parameter, but is determined by the Bohr-Sommerfeld quantization condition [17,18].

In the double-folding potential of Eq. (1), $\rho_{i=1,2}$ represent the density distributions of the daughter and the α clusters. As in previous studies [12,13,17–24], a two-parameter Fermi function is adopted for the former, while the latter is described by a Gaussian.

$$\rho_1(\mathbf{r_1}) = \frac{\rho_{1,s}}{1 + \exp\left(\frac{r_1 - R_d}{a}\right)}, \tag{3}$$

$$\rho_2(\mathbf{r_2}) = \rho_{2,s} \exp(-\beta {r_2}^2). \tag{4}$$

Here, both $\rho_{1,s}$ and $\rho_{2,s}$ are determined by normalizing the distributions to mass or charge number, with the radius parameter R_d taken to be $R_d = 1.07A^{1/3}$ fm and the diffuseness a fixed at $a = 0.54$ fm.

From Eq. (4), it is easy to recognize the size of the α cluster is controlled by the width parameter β. This parameter was taken as a typical value ($\beta = 0.7024$ fm^{-2}) that is determined by reproducing the experimental r.m.s. charge radius of a free α particle, i.e., the ^{4}He nucleus [33,35]. To use a constant β implies the α cluster remains as a compact entity of unchanged density distribution throughout the entire process, even when it appreciably overlaps with the daughter cluster. However, due to the nuclear mean field and the Pauli blocking effect, the α cluster inside nuclei is different from a free α particle [25,26]. As suggested in Ref. [25], the α cluster has a larger size inside the parent nucleus, and the medium effect manifests itself by changing the size of the α cluster during the α-decay process. Therefore, as an attempt to incorporate the nuclear medium effect, it is reasonable to introduce the matter-density dependence into the width parameter β. In other words, β should be treated as a function of daughter's density during the α emission process, i.e., $\beta = \beta[\rho_1(\mathbf{R})]$. Substituting it into Eq. (4), we obtain the α-cluster density distribution that is dependent on the center-of-mass (CM) position $\mathbf{R}$ of the α

cluster.

$$\rho_2(\mathbf{r_2},\mathbf{R}) = \rho_{2,s}\exp\left[-\beta(\mathbf{R}){r_2}^2\right]. \quad (5)$$

It should be noted that in Eq. (5) the LDA is employed to simplify the density dependence of β. This means the density distribution of the α cluster only depends on the matter density at a certain position $\mathbf{R}$, instead of a nonlocal density distribution. To determine the dependence on the latter requires the exact solution of the intrinsic cluster wave function in inhomogeneous nuclear matter, which will largely increase the complexity of the topic under study. Hence, in the present study, we adopt the LDA as in Refs. [25,26] and treat the β parameter as a function only dependent on the CM position $\mathbf{R}$ of the α cluster.

Given that the daughter nucleus is treated as the nuclear medium itself, from a many-body viewpoint, one might consider the density distribution of the daughter nucleus should also depend on the internuclear position $\mathbf{R}$. This means that $\rho_1(\mathbf{r_1})$ in Eq. (1) should be replaced by $\rho_1(\mathbf{r_1},\mathbf{R})$ due to the interactions with the α cluster. However, because the nucleons within the daughter nucleus are usually much more than those within the α cluster, the effect on the daughter's density distribution from the latter should be minor so that the dependence of ρ_1 on $\mathbf{R}$ is expected to be weak. Besides, features of this dependence have not been well understood, and a fixed density distribution (independent on $\mathbf{R}$) applied to the nuclear medium was considered to be a good approximation even in the many-body calculation of Refs. [25,26]. Hence, the form of $\rho_1(\mathbf{r_1})$ in Eq. (3) can be retained reasonably while considering the medium effect, and it is more important to focus on the determination of the density dependence of β, because it is known as the prominent manifestation of the nuclear medium effect.

With the medium effect incorporated into the α-cluster density distribution, the calculation of the nuclear potential in Eq. (1) can be further improved by using a density-dependent NN interaction. It is obvious that the presence of medium effect should not only affect the density of the α cluster but also the interaction between nucleons of the α cluster and the daughter nucleus. Therefore, instead of employing the density-independent M3Y interaction in Eq. (2), to use a density-dependent version of M3Y interaction would be more consistent to the main goal of present study. In the double-folding calculation of the improved α-nucleus potential, the CDM3Y6 version of NN interaction of the following form is employed:

$$t(E_\alpha,\mathbf{s},\rho_1,\rho_2) = \upsilon(\mathbf{s},E_\alpha)^{M3Y} f(\rho_1,\rho_2)g(E_\alpha), \quad (6)$$

with

$$f(\rho_1,\rho_2) = C[1+\alpha e^{-\beta(\rho_1+\rho_2)} - \gamma(\rho_1+\rho_2)], \quad (7)$$

$$g(E_\alpha) = 1 - 0.002E_\alpha/A_\alpha. \quad (8)$$

The parameters C, α, β, γ of this interaction are determined through reproducing the saturation properties of normal nuclear matter within Hartree-Fock calculations, and their values are given in Ref. [36]. Note that the CDM3Y6 NN interaction was confirmed to be valid for describing both the α-scattering experiments and the α-decay fine structure in previous studies [37,38]. Therefore, it should be appropriate for the double-folding model of the present study.

B. Determination of the density dependence for the α-cluster density distribution

In principle, the α-cluster density distribution in Eq. (5) should be obtained through solving the in-medium Schrödinger equation of the four-nucleon cluster. This was recently studied by Röpke *et al.* in Ref. [25], where explicit four-nucleon correlations and Pauli blocking are treated in a fully quantal formalism. By using a variational approach, they found numerically that the width b of the Gaussian-type trail wave function slowly decreases with increasing baryon density of the surrounding matter. Furthermore, compared with the value at zero-density limit, the width b is found to reduce by 20% at about 1/5 the saturation density $\rho_{1,s}$, i.e., the so-called Mott density $\rho^{\rm Mott}$ where the α cluster is formed. The reduction in b corresponds to an increase in the size of the α cluster inside the parent nucleus. Besides, it is easy to recognize that the square of parameter b in Ref. [25] is proportional to the parameter β in Eq. (5). Despite the density dependence of b is not analytically obtained so far, the above results still serve as a critical constraint to the variation of $\beta(\rho_1)$ at the surface region of low density.

Compared with the behavior of the α cluster at the nuclear surface, the α clustering in the interior of the parent nucleus is less well understood. According to previous research on nucleon correlations, it is suggested that the nucleons form an α cluster due to the strong α correlation established at the nuclear surface [30–32]. In the interior region where pairing takes the prominence, the nucleons appear as correlated pairs in the nuclear mean field, with the α-cluster configuration being substantially suppressed [27–29]. In Refs. [25,26], a similar scheme was employed to the cluster system above the Mott density $\rho^{\rm Mott}$, in which the four nucleons of the α cluster are described by simple shell-model states and thus become nonlocalized in the interior region. In the present work, both the four-nucleon distribution at $\rho_1 \geqslant \rho^{\rm Mott}$ and the α-cluster density distribution at $\rho_1 \leqslant \rho^{\rm Mott}$ are uniformly described by Eq. (5) as an approximation. This can be justified because the width parameter β will reduce with higher baryon density as is mentioned above. As a consequence, the Gaussian-type density distribution ρ_2 will be smoothed out, implying a situation that the four nucleons disperse within the parent nucleus. Therefore, it is reasonable in physics that a continuous $\beta(\rho_1)$ can be employed for the description of the medium effect under investigation.

Through refining the results of previous studies [25–32], we find the dependence of β on ρ_1 has to satisfy the following constraints:

(i) β should decrease smoothly with increasing baryon density, i.e., $\beta'(\rho_1) > 0$.
(ii) β should remain a positive value at the saturation density, i.e., $\beta(\rho_1 = \rho_{1,s}) > 0$.
(iii) At zero-density limit, β should equal to the experimental value for the free α particle, i.e., $\beta(0) = 0.7024\ \mathrm{fm}^{-2}$.

(iv) At one-fifth of the saturation density, the $\sqrt{\beta}$ reduces by 20% compared with its zero-density value, i.e., $\sqrt{\beta(\frac{1}{5}\rho_{1,s})} = \frac{4}{5}\sqrt{\beta(0)}$.

After a fair amount of trial, we propose a simple expression of $\beta(\rho_1)$ that fulfills the above conditions,

$$\beta(\rho_1) = \frac{0.7024}{1 + a_1\rho_1}, \tag{9}$$

where the coefficient a_1 is given by $a_1 = \frac{45}{16}\rho_{1,s}$. As is known, the nuclear saturation density is a very stable quantity, so the coefficient a_1 is almost a constant. It is emphasised that Eq. (9) is a generalization of the constant β ansatz in the conventional double-folding model, because the parameter β exactly restores to the typical value 0.7024 for the free α particle when the density ρ_1 approaches to zero. On the other hand, as the first attempt to incorporate the nuclear medium effect, Eq. (9) embodies all the critical features suggested in the previous researches, and thus adequately describes the density dependence of the α-cluster density distribution during the decay process. With the $\beta(\rho_1)$ determined, the double folding can be calculated by using Eq. (5). In this way, the nuclear medium effect is properly incorporated into the conventional double-folding model to generate an improved α-nucleus potential.

III. NUMERICAL RESULTS AND DISCUSSION

To obtain a pure manifestation of the nuclear medium effect in α decay, it is important to avoid the intervention of other structural properties such as deformation and angular momentum transfer during the calculation. Hence, it is better to start with the favored transitions of even-even spherical nuclei. We select the spherical α emitters from the recently updated deformation data (FRDM2012) [39], and take the decay energies from the latest atomic mass evaluation tables (AME2016) [40]. For spherical nuclei, the penetration possibility P can be evaluated in the semiclassical Wentzel-Kramers-Brillouin (WKB) approximation of enough accuracy,

$$P = \exp\left[-2\int_{R_2}^{R_3} k(R)dR\right], \tag{10}$$

where the wave number $k(R)$ is given by $k(R) = \sqrt{\frac{2\mu}{\hbar^2}|V(R) - Q_\alpha|}$. In the total α-nucleus potential $V(R)$, the Langer-modified centrifugal potential is included in addition to the double-folding nuclear and Coulomb potentials. Following the two-potential approach by Gurvitz *et al.* [41], the α-decay half-life is expressed as

$$T_{1/2} = \frac{\ln 2}{P_\alpha F \frac{\hbar}{4\mu} P}, \tag{11}$$

where P_α is the α-preformation factor and F is the normalization factor, given by

$$F^{-1} = \int_{R_1}^{R_2} \frac{dR}{k(R)} \cos^2\left[\int_{R_1}^{R} k(x)dx - \frac{\pi}{4}\right]. \tag{12}$$

It should be noted that the integrals of Eq. (10) and Eq. (12) are specialized by the three classical turning points R_1, R_2, and R_3.

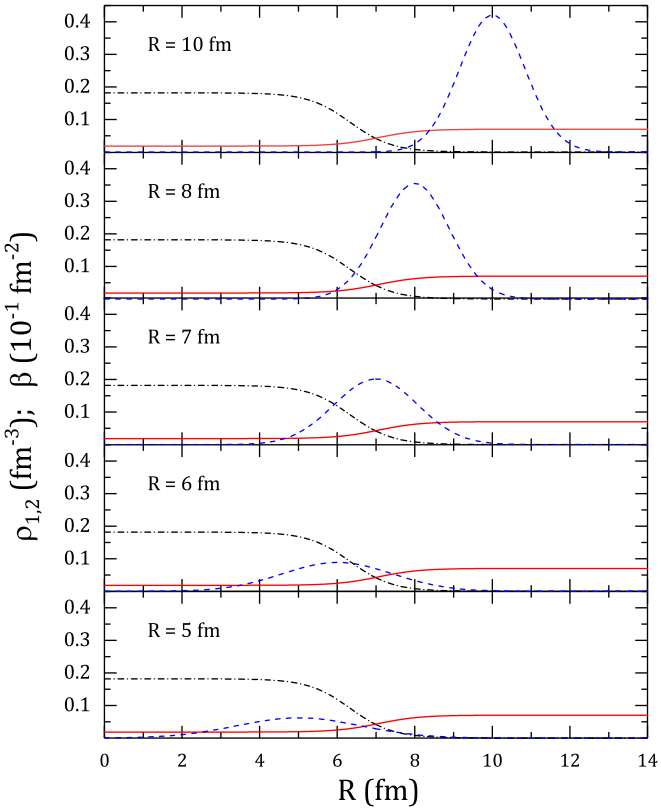

FIG. 1. The variation of the α-cluster density distribution with increasing overlap of the α and daughter clusters. The horizontal axis R represents the center-of-mass position of the α cluster. The blue dashed line and the black dot-dashed line are the density distributions of the α and the daughter clusters, respectively. The red solid line shows the variation of $\beta(R)$.

The penetration probability P is associated with the surface region of the α-nucleus potential, while the normalization factor F is responsible for the interior. Therefore, the medium effect on the α-nucleus potential can be estimated according to the variation of these two quantities.

To show the medium effect described by Eq. (9), the density distributions of the α and daughter clusters are plotted in Fig. 1. One can find the α-cluster density distribution dynamically changes as the overlap of the α and daughter clusters increases. At the zero-density region where the two clusters are isolated, ρ_2 becomes exactly the density distribution of a free α particle, reproducing the experimental r.m.s. charge radius as 1.67 fm. At 1/5 the saturation density where $R \approx 7$ fm, the width parameter β reduces to 0.4495 fm^{-2}, implying the r.m.s. charge radius increases to 1.99 fm inside the nuclei. Then, the density distribution becomes flattened while the α cluster is approaching the core region of higher density, where clustering usually appears as correlated pairs of nucleons and thus the spatial distribution of the four nucleons are approximated by a flat Gaussian function. Such an interesting process shows how the α cluster is softened by the increasing medium density, and it is consistent with the result given by many-body calculation in Ref. [25]. It is worth mentioning that a similar phenomenon was found recently in the analysis of the elastic $p + {}^{6,8}$He

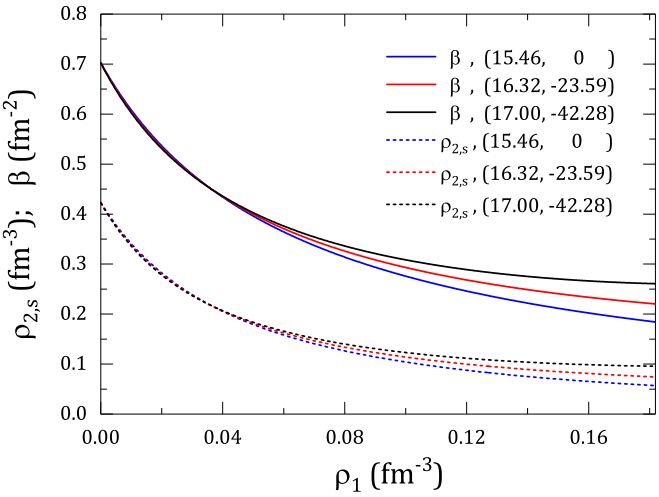

FIG. 2. The effect of the width parameter β on the peak density $\rho_{2,s}$ of the α-cluster density distribution. The legend shows the parameters (a_1, a_2) in the Eq. (13). Both β and $\rho_{2,s}$ smoothly decrease with increasing matter density. The minimum values of β and $\rho_{2,s}$ are reached at the saturation density which corresponds to the intercepts with the right border. The results indicates that the variation of $\beta_{\min}$ only slightly affects the α-cluster density distribution.

scattering, where the radius of the α cluster inside ^{6,8}He nuclei was also shown to be larger than that of the free α particle, due to its interaction with the halo neutrons [42].

Although Eq. (9) gives reasonably the trend and the critical features suggested in microscopic studies, it is easy to recognize that the minimum of width parameter β reached at the saturation density (i.e., $\beta_{\min} = \beta(\rho_{1,s})$) is already determined once a_1 is fixed. One should be careful that the value of $\beta_{\min}$ might also have a non-negligible influence on the resulting α-nucleus potential. A simple way to examine this speculation is to add a higher-order term to modify the value of $\beta_{\min}$,

$$\beta(\rho_1) = \frac{0.7024}{1 + a_1\rho_1 + a_2\rho_1^2}. \tag{13}$$

Note that Eq. (13) should also satisfy all the constraints for Eq. (9), so the chosen parameters a_1 and a_2 are not independent to each other. Taking the nucleus ^{212}Po as an example, we adjust the parameters to approximately give an identical interval between different $\beta_{\min}$, so that the influence to both the α-cluster density distribution (characterized by the peak density $\rho_{2,s}$) and the α-nucleus potential (characterized by the quantities F and P) can be clearly observed. As is shown in Fig. 2, both β and $\rho_{2,s}$ decrease with higher matter density, and the variation of $\beta_{\min}$ only slightly affects the value of $\rho_{2,s}$ at the saturation density. As to the improved α-nucleus potential (see Table I), the difference in the $\beta_{\min}$ causes a small variation in both F and P, implying that the effect can be reasonably ignored. However, if one compared the results with the case of constant β, it is easy to find the penetration probability P increases by about 55% due to the included medium effect. Therefore, one might safely conclude that the variation of $\beta_{\min}$ only has a minor effect on the α-nucleus potential, and it is sufficient to use Eq. (9) as a good approximation to the nuclear medium effect.

TABLE I. The effect of the different parameterized $\beta(\rho_1)$ on the α-nucleus potential. The parameters (a_1, a_2) of Eq. (13) are listed in the first two columns. The second and the third columns show the properties of the α-cluster density distribution at the saturation density: $\beta_{\min}$ (in fm^{-2}) and $\rho_{2,s}$ (in fm^{-3}). The last two columns are the normalization factor F (in m^{-2}) and the penetration probability P, whose variation reflects the effect on the α-nucleus potential. Note that row four shows the case of constant β where no medium effect is considered.

a_1	a_2	$\beta_{\min}$	$\rho_{2,s}$	F	P
15.46	0	0.1842	0.0568	5.97×10^{29}	5.28×10^{-15}
16.32	−23.59	0.2203	0.0743	6.55×10^{29}	5.28×10^{-15}
17.00	−42.28	0.2608	0.0957	6.68×10^{29}	5.41×10^{-15}
0	0	0.7024	0.4229	6.87×10^{29}	3.42×10^{-15}

To demonstrate the details of the nuclear medium effect, the total α-nucleus potential as well as its components of $\alpha + ^{208}$Pb system is plotted in Fig. 3. It can be found that the medium effect gives rise to an obvious transformation in the interior region of the nuclear potential while maintaining its depth. As is known, the internal geometry of the α-nuclear potential is critical to give correct energy levels, whereas α decay is more sensitive to the surface region where the Coulomb penetration happens [43]. In a recent study, researchers attempted to combine the good surface features described by the folded M3Y potential, and the more successful internal geometry of the Woods-Saxon (WS) potential (WS + WS^3-type), to achieve a unified description of the α-cluster structure in nuclei [44,45]. By fitting the parameters of WS + WS^3 potential to the surface part of

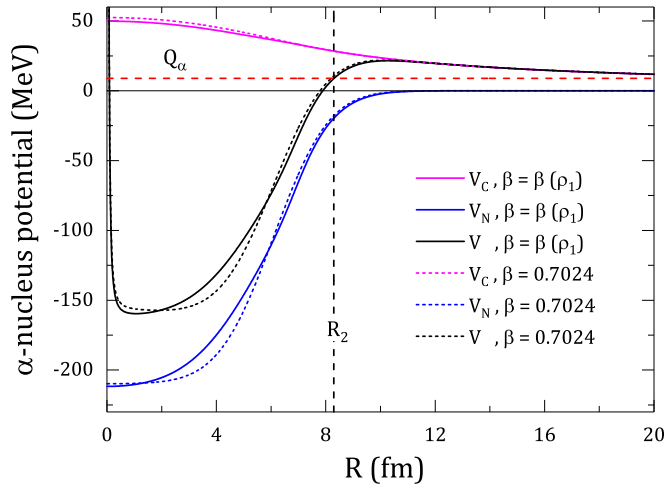

FIG. 3. The double-folding α-nucleus potential of the $\alpha + ^{208}$Pb system for the α decay of ^{212}Po. The Coulomb potential V_C, the nuclear potential V_N, and the total potential V are distinguished by different colors. The potentials with and without the medium effect are, respectively, denoted by the solid and dashed lines. The interior and the surface region of the α-nucleus potentials are separated by the second turning point R_2.

TABLE II. α-decay half-lives of spherical even-even nuclei around the shell closures. The experimental half-lives are given in the fifth column. The calculated half-lives $T_{1/2}^{\mathrm{Cal1}}$ (with the medium effect) and $T_{1/2}^{\mathrm{Cal2}}$ (without the medium effect) are shown in the sixth and the eighth columns (in second), respectively. We have adopted $P_\alpha = 1$ in the calculation so as to extract its empirical value from experimental data. The seventh and the ninth columns show the extracted P_α corresponding to $T_{1/2}^{\mathrm{Cal1}}$ and $T_{1/2}^{\mathrm{Cal2}}$.

α emitter	Q_α	$\rho_{1,s}$	a_1	$T_{1/2}^{\mathrm{Expt}}$	$T_{1/2}^{\mathrm{Cal1}}$	$P_\alpha^{(1)}$	$T_{1/2}^{\mathrm{Cal2}}$	$P_\alpha^{(2)}$
^{144}Nd	1.903	0.178	15.778	7.227×10^{22}	6.166×10^{22}	0.853	9.453×10^{22}	1.308
^{146}Sm	2.529	0.178	15.765	2.146×10^{15}	1.353×10^{15}	0.630	2.033×10^{15}	0.947
^{148}Gd	3.271	0.179	15.753	2.237×10^{9}	8.509×10^{8}	0.380	1.316×10^{9}	0.588
^{150}Dy	4.351	0.179	15.741	1.195×10^{3}	3.562×10^{2}	0.298	5.371×10^{2}	0.449
^{152}Er	4.934	0.179	15.729	1.144×10^{1}	3.508×10^{0}	0.306	5.507×10^{0}	0.481
^{156}Hf	6.029	0.179	15.706	2.371×10^{-2}	6.113×10^{-3}	0.258	9.324×10^{-3}	0.393
^{158}W	6.613	0.179	15.695	1.250×10^{-3}	3.663×10^{-4}	0.293	6.518×10^{-4}	0.521
^{182}Pb	7.066	0.181	15.579	5.612×10^{-2}	1.709×10^{-2}	0.304	2.647×10^{-2}	0.472
^{184}Pb	6.774	0.181	15.570	6.125×10^{-1}	1.792×10^{-1}	0.293	2.704×10^{-1}	0.441
^{186}Pb	6.470	0.181	15.562	1.205×10^{1}	2.456×10^{0}	0.204	3.795×10^{0}	0.315
^{188}Pb	6.109	0.181	15.554	2.699×10^{2}	7.248×10^{1}	0.269	1.118×10^{2}	0.414
^{190}Pb	5.698	0.181	15.546	1.775×10^{4}	5.193×10^{3}	0.293	8.142×10^{3}	0.459
^{192}Pb	5.221	0.181	15.538	3.559×10^{6}	1.433×10^{6}	0.403	2.217×10^{6}	0.623
^{194}Pb	4.738	0.181	15.530	8.795×10^{9}	1.033×10^{9}	0.118	1.630×10^{9}	0.185
^{196}Po	6.658	0.181	15.522	5.673×10^{0}	1.537×10^{0}	0.271	2.366×10^{0}	0.417
^{198}Po	6.310	0.181	15.515	1.853×10^{2}	3.727×10^{1}	0.201	6.348×10^{1}	0.343
^{200}Po	5.985	0.181	15.507	6.222×10^{3}	9.931×10^{2}	0.160	1.527×10^{3}	0.246
^{202}Po	5.701	0.181	15.500	1.394×10^{5}	2.038×10^{4}	0.146	3.101×10^{4}	0.222
^{204}Po	5.485	0.182	15.493	1.891×10^{6}	2.434×10^{5}	0.129	3.716×10^{5}	0.197
^{206}Po	5.327	0.182	15.486	1.395×10^{7}	1.597×10^{6}	0.115	2.499×10^{6}	0.179
^{208}Po	5.215	0.182	15.479	9.145×10^{7}	6.441×10^{6}	0.070	9.915×10^{6}	0.108
^{210}Po	5.408	0.182	15.472	1.196×10^{7}	5.150×10^{5}	0.043	7.881×10^{5}	0.066
^{212}Po	8.954	0.182	15.466	2.947×10^{-7}	5.442×10^{-8}	0.185	7.293×10^{-8}	0.247
^{214}Po	7.834	0.182	15.459	1.637×10^{-4}	4.812×10^{-5}	0.294	7.362×10^{-5}	0.450
^{216}Po	6.906	0.182	15.453	1.450×10^{-1}	5.442×10^{-2}	0.375	8.394×10^{-2}	0.579
^{206}Rn	6.384	0.182	15.486	5.487×10^{2}	1.358×10^{2}	0.248	1.987×10^{2}	0.362
^{208}Rn	6.261	0.182	15.479	2.356×10^{3}	4.009×10^{2}	0.170	6.189×10^{2}	0.263
^{210}Rn	6.159	0.182	15.472	9.000×10^{3}	1.078×10^{3}	0.120	1.662×10^{3}	0.185
^{212}Rn	6.385	0.182	15.466	1.434×10^{3}	1.020×10^{2}	0.071	1.580×10^{2}	0.110
^{214}Rn	9.208	0.182	15.459	2.700×10^{-7}	6.440×10^{-8}	0.239	9.019×10^{-8}	0.334
^{216}Rn	8.197	0.182	15.453	4.500×10^{-5}	2.408×10^{-5}	0.535	3.692×10^{-5}	0.820
^{210}Ra	7.151	0.182	15.472	4.167×10^{0}	8.792×10^{-1}	0.211	1.302×10^{0}	0.312
^{212}Ra	7.032	0.182	15.466	1.529×10^{1}	2.251×10^{0}	0.147	3.358×10^{0}	0.220
^{214}Ra	7.273	0.182	15.459	2.437×10^{0}	2.772×10^{-1}	0.114	4.189×10^{-1}	0.172
^{216}Ra	9.526	0.182	15.453	1.820×10^{-7}	5.015×10^{-8}	0.276	7.728×10^{-8}	0.425

folded M3Y potential, they obtained an improved α-nucleus potential, which incorporates the advantages of both potentials. Interestingly, we find a similar optimization of the α-nucleus potential can also be achieved by including the medium effect. As is shown in Fig. 3, with the medium effect included, the shape of the interior nuclear potential automatically transforms to a similar geometry as given by the WS + WS^3 potential; meanwhile, the surface region almost maintains the asymptotic behavior of the double-folding potential. Such an accidental finding appears to indicate that the absence of the nuclear medium effect is probably responsible for the blemish in the internal region of the conventional double-folding potential, which is desired to be investigated in the future. In terms of the result shown in Fig. 3, the transformation of the internal shape due to the included medium effect is considered favorable for a realistic double-folding α-nucleus potential.

For the surface region of relevance to α decay, the decline in both Coulomb and nuclear potentials due to the medium effect is subtle as shown in Fig. 3. However, such a minor variation is found to cause a 30% $\sim$ 40% decrease in the theoretical half-lives compared with the conventional calculation. In Table II, we list the results of favored α transitions of spherical even-even nuclei. $T_{1/2}^{\mathrm{Cal1}}$ represents the calculated half-lives with the consideration of nuclear medium effect, while $T_{1/2}^{\mathrm{Cal2}}$ is for the case of constant β. The experimental half-lives $T_{1/2}^{\mathrm{Expt}}$ are listed in the fifth column for reference. While calculating the half-lives, the α-preformation factors is usually taken as a fixed constant for a certain kind of nuclei in systematic calculations [17,18]. Because the investigated nuclei are almost located near either the proton or neutron shell closures, the variation of α-preformation factors between the adjacent nuclei would be more significant than in the open-shell region [24,46,47].

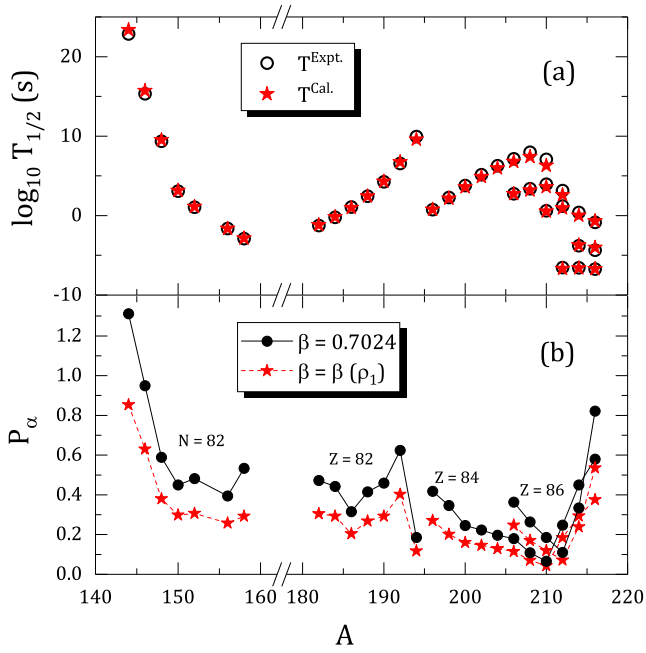

FIG. 4. (a) Comparison of the calculated half-lives with experimental data. (b) Variation of the α-preformation factors with mass number. The medium effect mainly leads to a general decrease in the magnitude of P_α factors, while a reasonable trend of the variation is maintained.

Therefore, to adopt a fixed P_α for different α transitions as in previous studies would be inappropriate here. To exclude the interference of this uncertain quantity, we have employed $P_\alpha = 1$ in our calculation to extract the empirical P_α value from the experimental half-lives. The extracted empirical P_α corresponding to the above two cases are given as $P_\alpha^{(1)}$ and $P_\alpha^{(2)}$.

As expected, the daughter's saturation density $\rho_{1,s}$ determined by the two-parameter Fermi distribution is very stable, which leads to an almost constant parameter a_1. This means the medium effect of different nuclei can be well approximated by an identical expression $\beta(\rho_1)$. Another feature in Table II is that, as a consequence of the medium effect, the reduction in the α-decay half-lives is systematical and substantially of approximate magnitudes. This corresponds to a decrease of the same order in the empirical P_α factors, which are extracted from the experimental half-lives. As is known, the P_α factor, which describes the preformation probability should always be less than unity according to its definition. However, it was found that the P_α given by the conventional double-folding α-nucleus potential are sometimes overestimated, for example, the $P_\alpha^{(2)} = 1.308$ of ^{144}Nd is obviously inappropriate. However, with the medium effect to be included, the obtained $P_\alpha^{(1)}$ strictly embodies this basic property, and the average value 0.258 of $P_\alpha^{(1)}$ is also strongly consistent with previous analyses [4,46]. Hence, this in turn justifies that the nuclear medium effect is essential to a precise description of the realistic α-nucleus interaction.

In order to generally evaluate the reliability of the improved α-nucleus potential, we demonstrate the variation of half-lives and preformation factors with mass number in Fig. 4. Since the exact P_α factors is not yet known, we take the average value 0.258 in the half-life calculation as a very rough estimation. However, we find the results still agree fairly well with the experimental data because a statistical analysis gives the deviation within a factor of 1.6. As for the empirical P_α factors, the results are connected according to different isotopic and isotonic chains, so that the evolution of P_α can be easily observed. As we can see, the medium effect mainly results in a decrease in the magnitude of the empirical P_α factors, whereas the trend is very similar to the conventional case. This indicates the medium effect does not make big differences to the trend of P_α variation, which is expectable because as a kind of averaged effect, it only generally affects the strength of the formation amplitude, while the trend is much more sensitive to the detailed nuclear structure differences. Note that in the present study the medium effect is approximated by a simple density-dependent $\beta(\rho_1)$ where local density is the only factor under consideration. To incorporate more structural details of the investigated nucleus, the β function should be associated with additional structural quantities and thus will become more sophisticated. This may be investigated in the future. It is worth mentioning that the P_α variation as an indicator of nuclear structural evolution was systematically investigated in previous studies [46,47]. As can be observed from the $Z = 84,86$ isotopic chains in Fig. 4(b), critical features such as the shell effect of P_α are reasonably reproduced, showing the good reliability of both α-nucleus potentials.

IV. SUMMARY

We introduce the nuclear medium effect into the widely used double-folding model to generate an improved α-nucleus potential. The density distribution of the α cluster is now considered to depend on its surrounding baryon density, as a kind of medium effect resulting from the variation of Pauli blocking. This density dependence is embedded into the width parameter β of the Gaussian-type density distribution, so that the α cluster smoothly reduces its size while moving outward the daughter's region. We extract the results from previous microscopic studies to constrain the density dependence of β, and a simple expression of $\beta(\rho_1)$ is proposed for the calculation of double-folding α-nucleus potential. The influence of the medium effect is investigated and discussed in details from the perspective of α decay.

The inclusion of medium effect brings about an favorable improvement in the conventional double-folding potential. For the interior region, the geometry of the potential obviously varies towards an preferable shape analogous to the Woods-Saxon type. In the surface region, the medium effect slightly reduces the potential, and at the same time maintains the good asymptotic behavior of double-folding potential. As a consequence to α decay, the half-lives of the investigated spherical nuclei generally reduce by 30% $\sim$ 40% compared with the conventional calculation. After the α-preformation factor is considered, the experimental half-lives are well reproduced by the improved α-nucleus potential. In addition, through deducing the empirical α-preformation factors from the improved potential, it is found that the medium effect mainly affects the magnitude of the preformation probability,

keeping the trend of P_α variation unchanged. With a general decrease in the deduced P_α, the importance of the medium effect is justified because the magnitude is more self-consistent with the definition of α-preformation factor.

In conclusion, through introducing the nuclear medium effect, we obtain an improved double-folding α-nucleus potential, which explains well the experimental α-decay data. More importantly, it is emphasized that the included medium effect enables the potential to incorporate more details of the α-decay process, especially the dynamic behavior of the α cluster at the nuclear surface. However, one should remember that the density dependence of the α-cluster density distribution is approximated in a phenomenological way. To go beyond the present study, it can be replaced by an exact density distribution, for which the analytical solution of the in-medium equation for the α intrinsic motion is required. On the other hand, the density distribution of the daughter nucleus in the present calculation is taken to be of the fixed Fermi shape as a typical approximation. One can also consider the medium effect on the daughter nucleus and thus its density distribution should be treated dynamically, analogous to the case for the α cluster. The possible importance of these factors to the α-nucleus potential requires a further investigation in the future.

ACKNOWLEDGMENTS

Z. Ren thanks Professor G. Röpke, Professor P. Schuck, and Professor H. Horiuchi for the helpful discussions. This work is supported by the National Natural Science Foundation of China (Grants No. 11535004, No. 11375086, No. 11120101005, No. 11175085, and No. 11235001), by the National Major State Basic Research and Development of China (Grant No. 2016YFE0129300), and by the Science and Technology Development Fund of Macau under the Grant No. 068/2011/A.

[1] S. Hofmann and G. Münzenberg, Rev. Mod. Phys. **72**, 733 (2000).
[2] Yu. Ts. Oganessian, J. Phys. G: Nucl. Part. Phys. **34**, R165 (2007).
[3] A. Astier, P. Petkov, M.-G. Porquet, D. S. Delion, and P. Schuck, Phys. Rev. Lett. **104**, 042701 (2010).
[4] K. Varga, R. G. Lovas, and R. J. Liotta, Phys. Rev. Lett. **69**, 37 (1992).
[5] D. Seweryniak, K. Starosta, C. N. Davids *et al.*, Phys. Rev. C **73**, 061301(R) (2006).
[6] R. D. Page, P. J. Woods, R. A. Cunningham, T. Davinson, N. J. Davis, A. N. James, K. Livingston, P. J. Sellin, and A. C. Shotter, Phys. Rev. C **53**, 660 (1996).
[7] A. N. Andreyev, M. Huyse, P. Van Duppen, L. Weissman *et al.*, Nature (London) **405**, 430 (2000).
[8] B. Buck, A. C. Merchant, and S. M. Perez, Phys. Rev. C **45**, 2247 (1992).
[9] P. Mohr, Phys. Rev. C **73**, 031301(R) (2006).
[10] V. Yu. Denisov and H. Ikezoe, Phys. Rev. C **72**, 064613 (2005).
[11] V. Yu. Denisov, O. I. Davidovskaya, and I. Yu. Sedykh, Phys. Rev. C **92**, 014602 (2015).
[12] D. N. Basu, J. Phys. G: Nucl. Part. Phys. **29**, 2079 (2003).
[13] C. Xu and Z. Ren, Nucl. Phys. A **753**, 174 (2005).
[14] D. S. Delion, S. Peltonen, and J. Suhonen, Phys. Rev. C **73**, 014315 (2006).
[15] G. Royer and H. F. Zhang, Phys. Rev. C **77**, 037602 (2008).
[16] N. G. Kelkar and H. M. Castañeda, Phys. Rev. C **76**, 064605 (2007).
[17] C. Xu and Z. Ren, Phys. Rev. C **74**, 014304 (2006).
[18] D. Ni and Z. Ren, Phys. Rev. C **81**, 024315 (2010).
[19] C. Xu and Z. Ren, Phys. Rev. C **75**, 044301 (2007).
[20] Y. Qian and Z. Ren, J. Phys. G: Nucl. Part. Phys. **39**, 115106 (2012).
[21] D. Ni, Z. Ren, T. Dong, and Y. Qian, Phys. Rev. C **87**, 024310 (2013).
[22] Y. Qian, Z. Ren, and D. Ni, Phys. Rev. C **89**, 024318 (2014).
[23] M. Ismail, A. Y. Ellithi, M. M. Botros, and A. Adel, Phys. Rev. C **81**, 024602 (2010).
[24] Y. Qian and Z. Ren, Sci. Chi. Phys. Mech. Astron. **56**, 1520 (2013).
[25] G. Ropke, P. Schuck, Y. Funaki, H. Horiuchi, Z. Ren, A. Tohsaki, C. Xu, T. Yamada, and B. Zhou, Phys. Rev. C **90**, 034304 (2014).
[26] C. Xu, Z. Ren, G. Ropke, P. Schuck, Y. Funaki, H. Horiuchi, A. Tohsaki, T. Yamada, and B. Zhou, Phys. Rev. C **93**, 011306(R) (2016).
[27] D. M. Brink and J. J. Castro, Nucl. Phys. A **216**, 109 (1973).
[28] H. Takemoto, M. Fukushima, S. Chiba, H. Horiuchi, Y. Akaishi, and A. Tohsaki, Phys. Rev. C **69**, 035802 (2004).
[29] G. Röpke, A. Schnell, P. Schuck, and P. Nozières, Phys. Rev. Lett. **80**, 3177 (1998).
[30] M. Girod and P. Schuck, Phys. Rev. Lett. **111**, 132503 (2013).
[31] T. Sogo, G. Ropke, and P. Schuck, Phys. Rev. C **81**, 064310 (2010).
[32] Z. Ren and G. Xu, Phys. Rev. C **36**, 456 (1987).
[33] G. R. Satchler and W. G. Love, Phys. Rep. **55**, 183 (1979).
[34] D. Ni and Z. Ren, Phys. Rev. C **82**, 024311 (2010).
[35] J. S. McCarthy, I. Sick, and R. R. Whitney, Phys. Rev. C **15**, 1396 (1977).
[36] D. T. Khoa, G. R. Satchler, and W. von Oertzen, Phys. Rev. C **56**, 954 (1997).
[37] D. T. Khoa, Phys. Rev. C **63**, 034007 (2001).
[38] D. Ni and Z. Ren, Phys. Rev. C **83**, 014310 (2011).
[39] P. Moller, A. J. Sierk, T. Ichikawa, and H. Sagawa, At. Data Nucl. Data Tables **109**, 1 (2016).
[40] M. Wang, G. Audi, F. G. Kondev *et al.*, Chin. Phys. C **41**, 030003 (2017).
[41] S. A. Gurvitz and G. Kalbermann, Phys. Rev. Lett **59**, 262 (1987).
[42] L. X. Chung, O. A. Kiselev, D. T. Khoa, and P. Egelhof, Phys. Rev. C **92**, 034608 (2015).
[43] R. G. Lovas, R. J. Liotta, A. Insolia, K. Varga, and D. S. Delion, Phys. Rep. **294**, 265 (1998).
[44] T. T. Ibrahim, S. M. Perez, and S. M. Wyngaardt, Phys. Rev. C **82**, 034302 (2010).
[45] B. Buck, A. C. Merchant, and S. M. Perez, Phys. Rev. C **51**, 559 (1995).
[46] D. Deng and Z. Ren, Phys. Rev. C **93**, 044326 (2016).
[47] R. Bonetti and L. Milazzo-Colli, Phys. Lett. B **49**, 17 (1974).